

# Control and Jetting Characteristics of an Innovative Jet Valve With Zoom Mechanism and Opening Electromagnetic Drive

Can Zhou, Junhui Li, Ji'an Duan, and Guiling Deng

**Abstract**—In order to develop jetting technology in LED and microelectronics packaging, an innovative electromagnetic jet valve with zoom mechanism and opening electromagnetic coil is suggested, and an improved method of double voltage drive is applied in the electromagnetic control. It is found that the needle stroke of the new jet valve is increased to 1.3 times, and the needle velocity is raised to 1.8 times, and the temperature of opening electromagnetic coil is lowered to 6.7 °C. The jet valve can successfully jet 4 Pa·s high-viscosity adhesives at room temperature due to the improvement of dynamic characteristics. It will provide a new method for jetting high-viscosity adhesives.

**Index Terms**—Double voltage drive, high-viscosity adhesive, jet valve, opening electromagnetic coil, zoom method.

## I. INTRODUCTION

With the development of science and technology, adhesives play a more significant role in modern industry. LED packaging, 3-D print and consumer electronics [1]–[7], and high-viscosity adhesive are widely used in the autoelectronics and LED industry. For example, the world production of LED industry reached \$576.6 billion in 2014. However, high-viscosity adhesives are always delivered by contact-based valve [8]–[12].

Adhesive distributing technology is grouped into contact-based dispensing and jet dispensing [13]–[16]. Compared with the contact-based dispensing, the features of jet dispensing include high quality, high flexibility, high reliability, high efficiency, and low cost [2]. A traditional jet valve cannot deliver high-viscosity adhesives at room temperature [17]–[20]. Pre-heating will lower the viscosity, which will also make adhesives go bad and decrease the performance. Besides, since the driving mode of single voltage, the common electromagnetic jet valve generates a great amount of heat.

Therefore, this study was undertaken to examine a novel electromagnetic jet valve developing high-viscosity adhesive jetting, and the jetting characteristics of the new electromagnetic jet valve are discussed.

Manuscript received May 24, 2015; revised July 18, 2015; accepted September 24, 2015. Date of publication September 28, 2015; date of current version February 24, 2016. Recommended by Technical Editor Z. Sun. This work was supported by the National Basic Research Program of China (973 program: 2011CB013104) and Fundamental Research Funds for Central Universities of Central South University (2013zzts034), China. (*Corresponding author:* Junhui Li.)

The authors are with the State Key Laboratory of High Performance Complex Manufacturing, School of Mechanical and Electrical Engineering, Central South University, Changsha 410083, China (e-mail: zhoucan@csu.edu.cn; lijunhui@csu.edu.cn; duanjian@csu.edu.cn; gldeng@csu.edu.cn).

Color versions of one or more of the figures in this paper are available online at <http://ieeexplore.ieee.org>.

Digital Object Identifier 10.1109/TMECH.2015.2482969

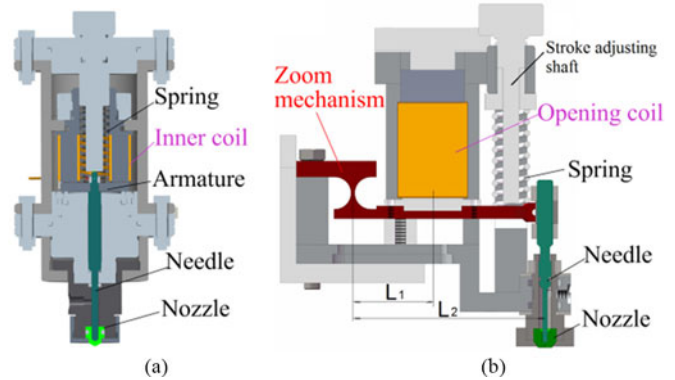


Fig. 1. Structure of electromagnetic jet valve. (a) is the common electromagnetic jet valve; (b) is the innovative electromagnetic jet valve with zoom mechanism and opening electromagnetic coil.

## II. PRINCIPLE AND CONTROL METHOD

### A. Novel Structure and Principle

The structure of the common electromagnetic jet valve is presented in Fig. 1(a), and the new structure is shown in Fig. 1(b). The zoom mechanism is a lever with a flexible hinge, which is introduced into the new structure to magnify the needle stroke of the new electromagnetic valve. Due to the zoom lever, the dynamic characteristics of needle and the jetting characteristics of the new jet valve will be improved.

When the dispenser is off work, the needle is pressed on the nozzle by a spring to prevent the adhesives leaking out. While the current is on, the high voltage make the electromagnet magnetize rapidly, and the electromagnetic force makes the armature moving upward. The zoom lever rotates around the center of the hinge with the armature. The needle moves upward with the lever and the spring is compressed at the same time. The stroke of the needle can be set by the adjusting shaft. Then, the low voltage makes the needle stays at the highest position for several microsecond (the valve opening time). It ensures that there is sufficient time for adhesives to be filled into the chamber of the nozzle. Then, the current is turned off and the electromagnetic force disappears. The needle moves downward rapidly. Elastic potential energy of the spring is converted to kinetic energy of the needle immediately. When the needle strikes on the nozzle, a dot of adhesives is jetted out and the whole cycle starts again.

Electromagnetic force can be calculated with

$$F = \frac{\mu \cdot s}{2} \cdot \left( \frac{NI}{k_f \delta} \right)^2 \quad (1)$$

where  $F$  is the electromagnetic force,  $\mu$  is permeability of vacuum,  $s$  is the cross-section area of the magnetic circuit,  $k_f$  is

magnetic flux leakage rate,  $\delta$  is the width of the gap,  $N$  is the turns of the coil, and  $I$  is the current.

At the same condition of current, turns of the coil and cross-section area, due to the zoom lever, the maximum stroke of the new valve needle is  $\sqrt{n}$  times as large as the common electromagnetic valve's ( $n$  is the magnification factor of the lever, which is the ratio of the force arms.  $n = L_1 : L_2$ . In this study,  $n = 2$ ). The stroke of the needle is amplified by the zoom mechanism. The dynamic characteristics of new jet valve in jetting stage are determined by

$$m\ddot{x} + c\dot{x} + kx = F_1 \quad (2)$$

where  $m$  is the equivalent mass of the needle. The mass of the lever, the needle, and the spring contribute to  $m$ . The greater distance to the flexible hinge center, the greater contribution to  $m$ .  $c$  is the equivalent damp. Damping of the system includes two parts: the first is the viscous damping of glue to the needle; the other part is damping between the lever and the stroke adjusting shaft.  $k$  is equivalent stiffness. The spring and the flexible hinge contribute to  $k$ .  $F_1$  is outer load and  $x$  is the displacement of the needle. Compared with the common electromagnetic jet valve,  $m$ ,  $c$ , and  $k$  of the new jet valve are nearly the same. The initial value of  $x$  is the stroke of the needle, which is  $\sqrt{n}$  times as large as the common electromagnetic valve's. The maximum  $\dot{x}$  will increase. The needle can obtain more kinetic energy in the jetting stage.

### B. Improved Control Method

The control scheme of electromagnetic jet valve is shown in Fig. 2(a). The pulse signal made by industrial computer is used to control the output of the drive circuit. The frequency and the duty circle of the controlling pulse signal determine the frequency and the opening time of the jet valve. The drive circuit can provide suitable voltage to drive the electromagnet. The drive circuit is extremely different between the common electromagnetic jet valve and the new one. The common electromagnetic jet valve is driven by single voltage pulse, and the new electromagnetic jet valve is driven by double voltage pulse. The outputting voltage amplitude of the drive circuit is determined by the power source.

The common electromagnetic jet valve is driven by single voltage pulse, which makes a great amount of heat. At the beginning of the working circle, since the gap between the armature and the core is large, high voltage is necessary for the electromagnetic jet valve to make the armature moving upward. When the gap becomes small, low voltage is enough to keep the armature at the position. In order to reduce heating power and ensure working steadily, the double voltage pulse is applied to drive the new electromagnetic jet valve. The waveforms of the single voltage and double voltage are presented, respectively, in Fig. 2(b) and (c). In this study,  $V$  is equal to  $V_1$ , since the new jet valve is designed to provide the same magnetic field strength as the common one at the beginning of the jet valve working circle.  $V_1$  is usually several times larger than  $V_2$ . In this experiment,  $V_1$  is 30 V, and  $V_2$  is 5 V. Apparently, for the same frequency and opening time, the power consumption and thermal power could be lowered due to the new driving method.

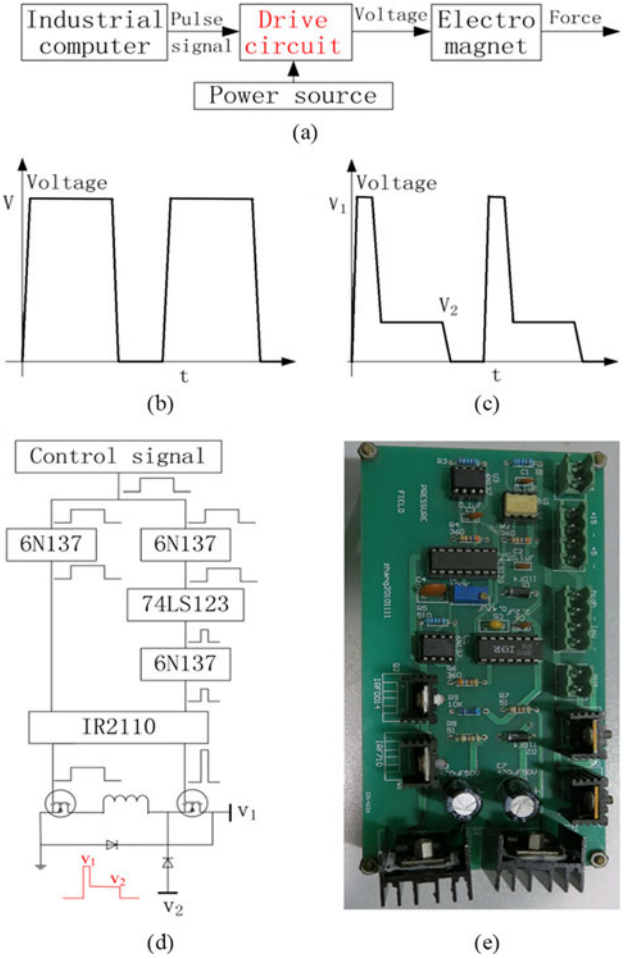


**Fig. 2.** (a) Control flow of electromagnetic jet valve, (b) single drive voltage waveform, (c) double drive voltage waveform, (d) the topological graph of drive circuit, and (e) the picture of the circuit of drive circuit.

In order to realize the double voltage waveform, a circuit is designed. The topological graph and the picture of the circuit are shown in Fig. 2(d) and (e). 6N137 is the type of the selected optical coupler, which is used to isolate the signals to prevent interference. A monostable trigger (74LS123) is selected to adjust the duty circle of the pulse. IR2110 is a metal-oxide-semiconductor field-effect transistor power driver, which works as a high-frequency switch. The square pulse is input, and corresponding high power double voltage pulse can be obtained by the circuit.

### C. Experimental Setup

To analyze the dynamic characteristics, thermal characteristics, and jet performance of the new jet valve, a jetting system and a testing system are designed as shown in Fig. 3. The jetting system consists of a new electromagnetic dispenser, a motion platform, a pneumatic system, and a software. The motion platform can make the new jet valve moving along X-, Y-, and Z-directions, and the motion is controlled by the software. The power source is used to supply the energy for the coil. The testing system includes a high-speed camera, laser distance sensor,

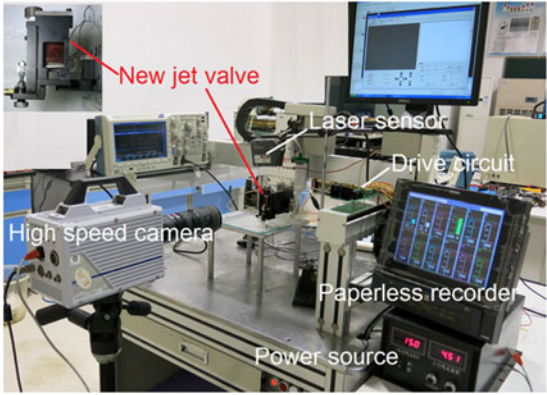


Fig. 3. Experimental setup.

temperature sensors, and a paperless recorder. The high-speed camera is used to record the jetting process of new valve, and the type of high-speed camera is Photon FASTCAM-SA1.1. The filming frequency of the high-speed camera is set to 5000 frames/s in the testing. Keyence LK-80 laser sensor and LK-G3001 controller are used to test the displacement of the needle. The sample frequency of the laser distance sensor is 50 kHz, and the accuracy of the selected laser sensor is  $0.2 \mu\text{m}$ . The velocity of the needle can be calculated as the difference of the displacement. Pt100 temperature sensor is used to test the temperature of the jet valve. ENVADA EN880C-D-12 paperless recorder is used to record the temperature data.

### III. RESULTS AND DISCUSSION

The needle displacement of the jet valves is shown in Fig. 4(a). The needle displacement of the new electromagnetic jet valve reaches to 0.53 mm. The needle displacement of the common electromagnetic jet valve is 0.4 mm. The needle displacement of the new jet valve is about 1.3 times larger than the common jet valve's.

The needle velocity curves of the jet valves is shown in Fig. 4(b). The maximum upward velocity of the new electromagnetic jet valve is 0.6 m/s, and the common one's is 0.45 m/s. The maximum upward velocity is about 1.3 times larger than the common one's. The maximum downward velocity of the new electromagnetic jet valve is 0.78 m/s, and the common one's is 0.43 m/s. The maximum downward velocity is about 1.8 times larger than the common one's. Due to the zoom lever, the dynamic characteristics of the new electromagnetic jet valve are improved significantly.

On the one hand, the stroke of the new jet valve is improved. On the other hand, as the contribution of the flexible hinge, the stiffness of the new jet valve is larger. The new valve system can store more elastic potential energy. When the needle moves downward, the potential energy transforms into kinetic energy. Compared with the common jet valve, the increment of the kinetic energy is more than the increment of the equivalent mass  $m$ . So, the maximum downward velocity is improved.

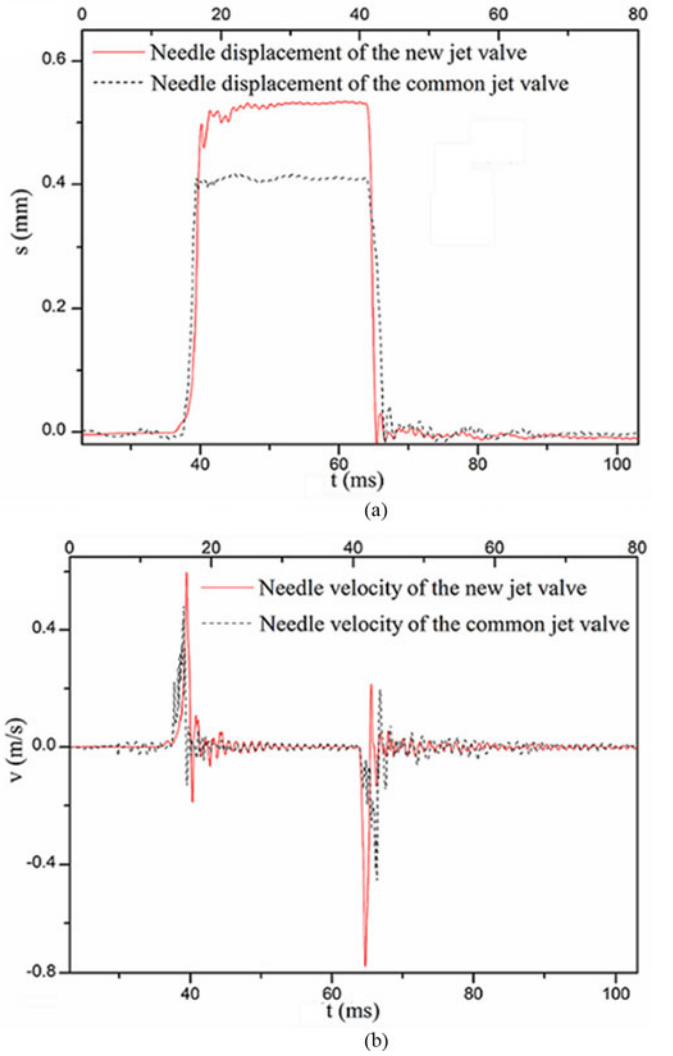


Fig. 4. (a) Displacement of the needle from, and (b) velocity of the needle from.

The temperature rising curves of electromagnets are shown in Fig. 5 when the jet valves work. After 30 min working, the new electromagnetic jet valve reaches a new temperature balance, and the electromagnet temperature of the new jet valve is  $33^\circ\text{C}$ . The common electromagnetic jet valve rises to a new temperature balance, and the electromagnet temperature of the common jet valve increases to  $39.7^\circ\text{C}$ . The temperature increase of the new jet valve is only  $7^\circ\text{C}$ , and the temperature increase of the common jet valve reaches  $14.7^\circ\text{C}$ . When the two electromagnetic jet valves reach temperature balance stage, the new jet valve feels warm; however, the common one feels hot.

The double voltage driving method can decrease the power assumption and thermal power of the new valve. The opening structure of the new valve makes the heat fast dissipating. So, the temperature increase of the new valve was obviously lower than the common one. The reliability test shows that the life span of the new jet valve is more than 50 million times.

The jetting process of 4.0 Pa·s high-viscosity adhesives recorded by the high-speed camera is shown in Fig. 6. It

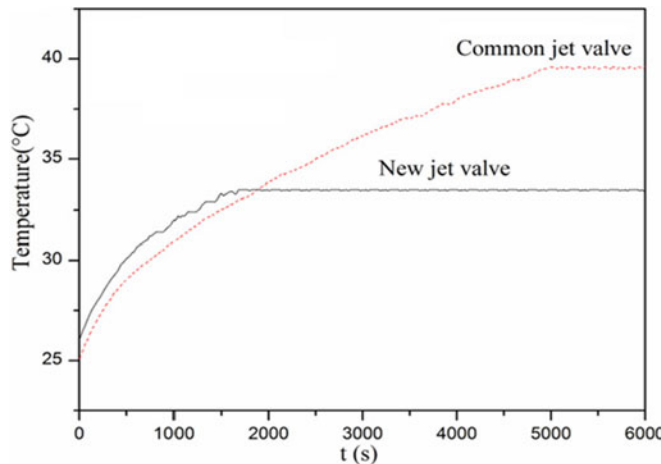


Fig. 5. Temperature of electromagnets.

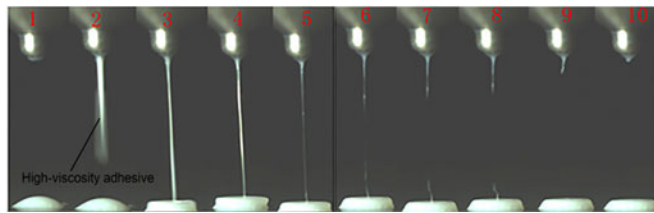


Fig. 6. Jetting process of 4.0 Pa·s high-viscosity adhesives.

confirms that the high-viscosity adhesives can be successfully delivered by the new jet valve, and the jetting process can be observed clearly through these pictures. The first image depicts the preparing stage of the new valve. The second and the third images show that the fluid is just jet out from the nozzle. Following, the fourth image depicts the neck of filament appears. Then, the fifth image shows the radius of the filament becoming extremely smaller. The sixth image shows the filament breaks off. The seventh, eighth, and ninth images depict the droplet at the bottom forms the dot and recoil goes back to the nozzle and the last picture presents the end of the jetting stage.

#### IV. CONCLUSION

In conclusion, with the help of the zoom mechanism, the dynamic characteristics of the new jet valve were improved significantly and the 4 Pa·s high-viscosity adhesives can be delivered without preheating. The double voltage driving method can decrease the power assumption and thermal power of the new valve. The opening structure of the new valve makes the heat fast dissipating and being easily observed when the valve is working. The temperature increase of the new valve was 7.7°C lower than the common one's, when the jet valves work.

It also reveals that zoom mechanism can be introduced to electromagnetic driving system for improving the dynamic characteristics, and double voltage driving method can decrease the power assumption and thermal power in electromagnetic application. The new electromagnetic jet valve will provide a

new method and principle for jetting high-viscosity adhesives in autoelectronics, LED industry, and electronics packaging industry.

#### REFERENCES

- [1] Y. Chu, C. Chen, and C. Tsou, "A silicon-based led packaging substrate with an island structure for phosphor encapsulation shaping," *IEEE Trans. Compon. Packag. Manuf. Technol.*, vol. 5, no. 2, pp. 155–162, Feb. 2015.
- [2] H. X. Li, J. Liu, C. P. Chen, and H. Deng, "A simple model-based approach for fluid dispensing analysis and control," *IEEE/ASME Trans. Mechatron.*, vol. 12, no. 4, pp. 491–503, Aug. 2007.
- [3] Y. Kwon and W. Kim, "Development of a new high-resolution angle-sensing mechanism using an RGB sensor," *IEEE/ASME Trans. Mechatron.*, vol. 19, no. 5, pp. 1707–1715, Oct. 2014.
- [4] H. Nasibov, A. Kholmatov, B. Akselli, A. Nasibov, and S. Baytaroglu, "Performance analysis of the CCD pixel binning option in particle-image velocimetry measurements," *IEEE/ASME Trans. Mechatron.*, vol. 15, no. 4, pp. 527–540, Aug. 2010.
- [5] M. Hashemi and X. B. Chen, "Theoretical investigation into the performance of the rotary-screw fluid dispensing process," *Trans. Can. Soc. Mech. Eng.*, vol. 32, nos. 3/4, pp. 325–331, 2008.
- [6] X. Ren, Q. Zhang, K. Liu, H. Li, and J. G. Zhou, "Modeling of pneumatic valve dispenser for printing viscous biomaterials in additive manufacturing," *Rapid Prototyping J.*, vol. 20, no. 6, pp. 434–443, 2014.
- [7] C. Huang, "Innovative parametric design for environmentally conscious adhesive dispensing process," *J. Intell. Manuf.*, vol. 26, no. 1, pp. 1–12, 2015.
- [8] Y. P. Hong and H. X. Li, "Comparative study of fluid dispensing modeling," *IEEE Trans. Electron. Packag. Manuf.*, vol. 26, no. 4, pp. 273–280, Oct. 2003.
- [9] K. Li, G. Tian, L. Cheng, A. Yin, W. Cao, and S. Crichton, "State detection of bond wires in IGBT modules using eddy current pulsed thermography," *IEEE Trans. Power Electron.*, vol. 29, no. 9, pp. 5000–5009, Sep. 2014.
- [10] L. Wang, J. Du, Z. Luo, X. Du, Y. Li, J. Liu, and D. Sun, "Design and experiment of a jetting dispenser driven by piezostack actuator," *IEEE Trans. Compon. Packag. Manuf.*, vol. 3, no. 1, pp. 147–156, Jan. 2013.
- [11] H. Xu, I. Qin, H. Clauberg, B. Chylak, and V. L. Acoff, "Behavior of palladium and its impact on intermetallic growth in palladium-coated cu wire bonding," *Acta Mater.*, vol. 61, no. 1, pp. 79–88, 2013.
- [12] M. Simi, M. Silvestri, C. Cavallotti, M. Vatteroni, P. Valdastri, A. Menciassi, and P. Dario, "Magnetically activated stereoscopic vision system for laparoendoscopic single-site surgery," *IEEE/ASME Trans. Mechatron.*, vol. 18, no. 3, pp. 1140–1151, Jun. 2013.
- [13] J. Li and G. Deng, "Technology development and basic theory study of fluid dispensing—A review," in *Proc. IEEE 6th CPMT Conf. High Density Microsyst. Des. Packag. Failure Anal.*, 2004, pp. 198–205.
- [14] C. Clasen, P. M. Phillips, L. Palangetic, and J. Vermant, "Dispensing of rheologically complex fluids: The map of misery," *AIChE J.*, vol. 58, no. 10, pp. 3242–3255, 2012.
- [15] Y. Kwon and W. Kim, "Development of a new High-resolution angle-sensing mechanism using an RGB sensor," *IEEE ASME Trans. Mechatron.*, vol. 19, no. 5, pp. 1707–1715, Oct. 2014.
- [16] X. Shu, H. Zhang, H. Liu, D. Xie, and J. Xiao, "Experimental study on high viscosity fluid micro-droplet jetting system," *Sci. China Technol. Sci.*, vol. 53, pp. 182–187, 2010.
- [17] A. D. Deshpande, X. Zhe, M. J. V. Weghe et al., "Mechanisms of the anatomically correct testbed hand," *IEEE-ASME T. Mech.*, vol. 18, no. 1, pp. 238–250, Feb. 2013.
- [18] S. Kim, B. Cook, T. Le, J. Cooper, H. Lee, V. Lakafosis, R. Vyasa, R. Moro, M. Bozzi, A. Georgiadis, A. Collado, and M. M. Tentzeris, "Inkjet-printed antennas, sensors and circuits on paper substrate," *IET Microw. Antenna Propag.*, vol. 7, no. 10, pp. 858–868, 2013.
- [19] S. B. Bammesberger, S. Kartmann, L. Tanguy, D. Liang, K. Mutschler, A. Ernst, R. Zengerle, and P. Kolay, "A low-cost, normally closed, solenoid valve for non-contact dispensing in the sub-mu l range," *Micromachines*, vol. 4, no. 1, pp. 9–21, 2013.
- [20] S. Lee and J. Kim, "Development and characterization of a cartridge-type pneumatic dispenser with an integrated backflow stopper," *J. Micromech. Microeng.*, vol. 20, no. 1, p. 015011, 2010.